

# A study on the exotic state $P_c(4312)$ , $P_c(4440)$ , $P_c(4457)$ in $pp$ collisions at $\sqrt{s} = 7, 13$ TeV

Chun-hui Chen<sup>1</sup>, Yi-Long Xie<sup>1</sup>, Hong-ge Xu<sup>1</sup>, Zhen Zhang<sup>2</sup>, Dai-Mei Zhou<sup>2</sup>, Zhi-Lei She<sup>1</sup>, Gang Chen<sup>\*1</sup>

<sup>1</sup> *School of Mathematics and Physics, China University of Geoscience, Wuhan 430074, China*

<sup>2</sup> *Institute of Particle Physics, Huazhong Normal University, Wuhan 430082, China*

The exotic resonant state  $P_c^\pm(4312)$ ,  $P_c^\pm(4440)$ , and  $P_c^\pm(4457)$  are studied by using the dynamically constrained phase space coalescence(DCPC) model and PACIAE model in  $pp$  collisions at  $\sqrt{s} = 7, 13$  TeV, respectively. We consider exotic state  $P_c^\pm(4312)$ ,  $P_c^\pm(4440)$  and  $P_c^\pm(4457)$  to be three kinds of possible structures, i.e. pentaquark state, the nucleus-like state, and the molecular state based on  $P_c^\pm \rightarrow J/\psi p(\bar{p})$  bound state. The yield, the transverse momentum distribution and the rapidity distribution of  $P_c$  with three different structures are all predicted. The results indicated that the yield is on the order of  $10^{-6}$ , which might provide reference for experimental research.

PACS numbers: 25.75.-q, 24.85.+p, 24.10.Lx

## I. INTRODUCTION

Quantum chromodynamics (QCD) as the fundamental theory of the strong interactions, specifies that quarks are bound in color-neutral hadrons with various structures. In the conventional quark model, a meson is made up a quark-antiquark pair and a baryon is made of three quarks. However, there exist some other interpretations for baryon structures which allows more complex structure such as multiquark states [1], hadronic molecules [2] hybrid states [3, 4] and glueball [5]. These complex structures are called exotic state hadrons. Exotic hadrons will continuously be a central topic in hadron physics.

In the last few years, various exotic state hadrons are observed in high energy collision experiments [6, 7], are called the XYZ particles. Particularly in 2015, LHCb Collaboration [8] reported two hidden-charm pentaquarks, i.e.  $P_c^+(4450)$  and  $P_c^+(4380)$  in the  $J/\psi p$  invariant mass distribution of the decaying  $\Lambda_B \rightarrow K^- J/\psi p$ .  $P_c^+(4450)$  showed up a narrow peak in distribution with a width of  $39 \pm 5 \pm 19$  MeV and  $P_c^+(4380)$  showed up another peak with a width of  $205 \pm 18 \pm 86$  MeV. In 2019 [9], LHCb Collaboration updated their measurement and observed the narrow peak  $P_c(4450)$  were separated into two narrow overlapping peaks,  $P_c^+(4440)$  and  $P_c^+(4457)$ , with a width of  $20.6 \pm 4.9_{-10.1}^{+8.7}$  and  $6.4 \pm 2.0_{-1.9}^{+5.7}$ , respectively. Meanwhile, the third peak  $P_c^+(4312)$  shows up and  $P_c^+(4380)$  are too small to be observed.

$P_c$  states have minimal quark content  $duu\bar{c}\bar{c}$ . For the two hidden-charm pentaquarks, there are different theoretical interpretations: the loosely bound meson-baryon molecular states [10–12], the tightly bound pentaquark states [13], and the hadrocharmonium states [14]. The  $P_c$  states with narrow peaks are under the threshold of binding energies of  $\Sigma_c^+ \bar{D}^0$ ,  $\Sigma_c^+ \bar{D}^{*0}$ , which makes the bound states of baryon and meson possible [9]. Hence we sug-

gest that the  $P_c$  states could be interpreted as the bound states of  $J/\psi p(\bar{p})$  [15]. Similar to Ref. [16] we also treated  $P_c(4312)$ ,  $P_c(4440)$  and  $P_c(4457)$  as three structures, i.e. pentaquark state, nucleus-like state and molecular state, according to the different distances of corresponding components.

In this paper, we study  $P_c^\pm$  states through decaying  $P_c^\pm \rightarrow J/\psi p(\bar{p})$  by using Monte Carlo simulation [17] approach in  $pp$  collisions at  $\sqrt{s} = 7, 13$  TeV. As the first step, the parton and hadron cascade model (PACIAE) [18] is used to generate the hadronic final state, including  $J/\psi$  and  $p(\bar{p})$ ; then the  $P_c(4312)$ ,  $P_c(4440)$  and  $P_c(4457)$  states yield, as well as the transverse momentum distribution and the rapidity distribution are predicted by a dynamically constrained phase-space coalescence(DCPC) model [19]. Here we will study three different configurations of the  $P_c$  state namely pentaquark state, nucleus-like state and molecular state.

## II. PACIAE MODEL AND DCPC MODEL

The parton and hadron cascade model PACIAE [18] is based on PYTHIA 6.4 [17] to describing various relativistic collision modes, such as relativistic  $pp$ ,  $\bar{p}p$ ,  $\bar{e}e$  collisions, and relativistic nuclear collisions (A-A and p-A). The PACIAE model is composed of four main stages: parton initiation, parton rescattering, hadronization, and hadron rescattering.

In order to produce the parton initial state, the string fragmentation [18] is temporarily turned off in PACIAE and breaks up the diquarks (anti-diquarks) to produce some matter composed by quarks anti-quarks and gluon. The parton rescattering is followed which depend on the  $2 \rightarrow 2$  LO-pQCD parton-parton cross sections [20]. After all parton rescatterings, hadronization of the final state partons are computed by the string fragmentation [18] or the Monte Carlo coalescence model [17]. The last stage is hadron rescattering process happening among two-body collision until the hadronic freeze-out.

In this paper, the yields of bound states are usually calculated in two steps. First, the final state hadrons are

\*Corresponding Author: chengang1@cug.edu.cn

calculated by the PACIAE model. Then, the bound states or exotic states are combined by the DCPC model[19]. The DCPC model is developed to calculate production of the bound states or exotic states after the final state particles produced by the PACIAE model [18] in  $pp$  collisions.

From quantum statistical mechanics [21], one can not precisely define both position  $\vec{q} \equiv (x, y, z)$  and momentum  $\vec{p} \equiv (p_x, p_y, p_z)$  of a particle in six-dimensional phase space because of the uncertainty principle,  $\Delta\vec{q}\Delta\vec{p} \sim h^3$ . One can only say this particle lies somewhere within a six-dimensional quantum box or state of volume of  $\Delta\vec{q}\Delta\vec{p}$  volume element in the six-dimensional phase space corresponds to a state of the particle. So we can estimate the yield of a single particle [21] by

$$Y_1 = \int_{E_A \leq H \leq E_B} \frac{d\vec{q}d\vec{p}}{h^3}, \quad (1)$$

where  $H$  and  $E_A$ ,  $E_B$  represent the energy function (Hamiltonian) and the energy threshold of the particle, respectively. The variables  $\vec{p}$  and  $\vec{q}$  are the coordinates and momentum of the particle in the center-of-mass frame at the moment after the hadronic freeze-out. Furthermore, the yield of  $N$  particles clusters can be calculated by the following integral:

$$Y_N = \int \dots \int_{E_A \leq H \leq E_B} \frac{d\vec{q}_1 d\vec{p}_1 \dots d\vec{q}_N d\vec{p}_N}{(h)^{3N}}. \quad (2)$$

Therefore, the yield of a  $P_c(4312)$ ,  $P_c(4440)$  and  $P_c(4457)$  consisting of  $J/\psi p(\bar{p})$  cluster in the DCPC model can be calculated by

$$Y_{P_c^\pm \rightarrow J/\psi p(\bar{p})} = \int \dots \int \delta_{12} \frac{d\vec{q}_{p(\bar{p})} d\vec{p}_{p(\bar{p})} d\vec{q}_{J/\psi} d\vec{p}_{J/\psi}}{h^6}, \quad (3)$$

$$\delta_{12} = \begin{cases} 1 & \text{if } 1 \equiv p(\bar{p}), 2 \equiv J/\psi; \\ m_0 - \Delta m \leq m_{inv} \leq m_0 + \Delta m; \\ q_{12} \leq R_0; \\ 0 & \text{otherwise.} \end{cases} \quad (4)$$

where,

$$m_{inv} = \sqrt{(E_{p(\bar{p})} + E_{J/\psi})^2 - (\vec{p}_{p(\bar{p})} + \vec{p}_{J/\psi})^2}. \quad (5)$$

Where  $m_0$  denotes the rest mass of  $P_c$  states,  $\Delta m$  refers to its mass uncertainty,  $q_{12} = |\vec{q}_1 - \vec{q}_2|$  represents the distance between the two particles  $p$  or  $\bar{p}$  and  $J/\psi$ . The dynamic constraint  $E_A \leq H \leq E_B$  in Eq.1 is replaced by the  $m_0 - \Delta m \leq m_{inv} \leq m_0 + \Delta m$ . The rest masses of  $P_c(4312)$ ,  $P_c(4440)$  and  $P_c(4457)$  were  $m_0 = 4311.9, 4440.3, 4457.3$  MeV/c<sup>2</sup> [15], respectively.

$P_c(4312)$ ,  $P_c(4440)$  and  $P_c(4457)$  is constructed by the combination of hadrons  $p(\bar{p})$  and  $J/\psi$  after the final hadrons have been produced by PACIAE model in  $pp$  collisions at  $\sqrt{s} = 7, 13$  TeV. According to the different distances  $q_{12}$  between  $p(\bar{p})$  and  $J/\psi$ , the exotic state  $P_c$  can be divided three structures: the pentaquark refers  $R_0 < 0.9$  fm, the nuclear-like state refers  $0.9 \leq R_0 < 1.91$  fm, and the molecular state refers  $R_0 \geq 1.91$  fm [15, 22].

### III. RESULTS

First, the multiparticle final state are produces using the PACIAE model in  $pp$  collisions at  $\sqrt{s} = 7, 13$  TeV. In addition to the  $K$  factor and parameters  $\text{parj}(1)$ ,  $\text{parj}(2)$ , and  $\text{parj}(3)$ , the other model parameters are fixed on the default values given in the PYTHIA model. In this model,  $\text{parj}(1)$  is the suppression of diquark-antidiquark pair production compared with quark-antiquark production,  $\text{parj}(2)$  is the suppression of strange quark pair production compared with up or down pair production, and  $\text{parj}(3)$  is the extra suppression of strange diquark production compared with the normal suppression of strange quark [18]. We determine the  $K$  factor,  $\text{parj}(1,2,3)$  for primary hadrons in PACIAE model by fitting to the LHCb and ALICE data of  $J/\psi$ ,  $p$  and  $\bar{p}$  [23, 24]. The fitted values of  $K = 0.9$ ,  $\text{parj}(1) = 0.13$ ,  $\text{parj}(2) = 0.20$ , and  $\text{parj}(3) = 0.90$  for  $pp$  collisions are used in later calculations.

Table I shows the yield of  $p(\bar{p})$  and  $J/\psi$  calculated with  $|y| < 0.5$ ,  $0.6 < p_T < 6$  GeV/c for  $p(\bar{p})$  and  $2.0 < y < 4.5$ ,  $0 < p_T < 14$  GeV/c for  $J/\psi$ , separately. Obviously the results of the PACIAE model are consistent with the data measured by LHCb Collaboration and ALICE Collaboration [23, 24].

TABLE I: The yield of particles ( $p$  or  $\bar{p}$  and  $J/\psi$ ) in  $pp$  collisions at  $\sqrt{s} = 7$  TeV simulated by the PACIAE model, and compared with data from LHCb Collaboration and ALICE Collaboration as the  $|y| < 0.5$ ,  $0.6 < p_T < 6$  GeV/c for  $p(\bar{p})$  and  $2.0 < y < 4.5$ ,  $0 < p_T < 14$  GeV/c for  $J/\psi$ , respectively [23, 24]. Here,  $J/\psi$  is from b decay and prompt production.

| particles | Experiment data                            | PACIAE                             |
|-----------|--|------------------------------------|
| $J/\psi$  | $(1.64 \pm 0.007 \pm 0.22) \times 10^{-4}$ | $(1.680 \pm 0.002) \times 10^{-4}$ |
| $p$       | $0.124 \pm 0.009$                          | $0.123 \pm 0.001$                  |
| $\bar{p}$ | $0.123 \pm 0.010$                          | $0.122 \pm 0.001$                  |

Then, we generate the event final states including  $p(\bar{p})$  and  $J/\psi$  using the PACIAE model in  $pp$  collisions at  $\sqrt{s} = 7, 13$  TeV, with the  $|y| < 3$ ,  $0 < p_T < 10$  GeV/c. Inputting  $J/\psi$  and  $p(\bar{p})$  into the DCPC model, the exotic states  $P_c$  are combined to generate by constructing  $J/\psi p(\bar{p})$  clusters, which can be considered as the exotic states  $P_c(4312)$ ,  $P_c(4440)$  and  $P_c(4457)$ . Here,  $J/\psi$  is from all  $J/\psi$  sources. We assume that there are three structures of  $P_c$  states [16]: pentaquark state, nucleus-like state and molecular state, which are denoted as  $P_{cp}$ ,  $P_{cn}$  and  $P_{cm}$ , respectively.

Fig.1 shows the yield of exotic state  $P_c^\pm(4312)$ ,  $P_c^\pm(4440)$  and  $P_c^\pm(4457)$  for three structures varying with parameter  $\Delta m$  from 0 to 20 MeV/c in  $pp$  collisions at  $\sqrt{s} = 7, 13$  TeV. It can be seen that the yield distribution patterns of exotic state  $P_c^\pm(4312)$ ,  $P_c^\pm(4440)$  and  $P_c^\pm(4457)$  for the three structures are all similar, which increases linearly as  $\Delta m$  increases. Meanwhile, under the same  $\Delta m$  and energy, the yields of exotic states with the nucleus-like structure are always larger than those with

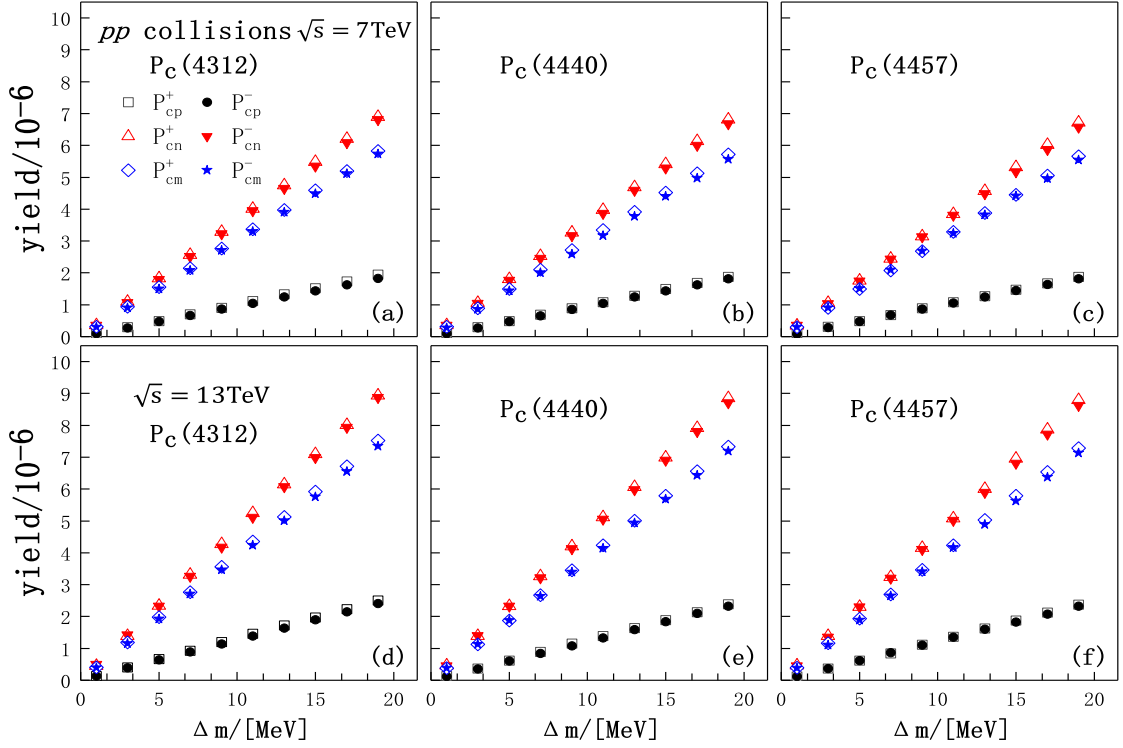


FIG. 1: The distribution of the yield of exotic states  $P_c^\pm(4312)$ ,  $P_c^\pm(4440)$ , and  $P_c^\pm(4457)$  with three structures ( $P_{cp}$ ,  $P_{cn}$ ,  $P_{cm}$ ) in  $pp$  collisions at  $\sqrt{s} = 7, 13$  TeV, as a function of mass uncertainty  $\Delta m$ . The data are computed by using PACIAE+DCPC model based on the  $J/\psi p(\bar{p})$  bound state. (a) as exotic states  $P_c^\pm(4312)$  at  $\sqrt{s} = 7$  TeV, (b) as exotic states  $P_c^\pm(4440)$  at  $\sqrt{s} = 7$  TeV, (c) as exotic states  $P_c^\pm(4457)$  at  $\sqrt{s} = 7$  TeV, (d) as exotic states  $P_c^\pm(4312)$  at  $\sqrt{s} = 13$  TeV, (e) as exotic states  $P_c^\pm(4440)$  at  $\sqrt{s} = 13$  TeV, (f) as exotic states  $P_c^\pm(4457)$  at  $\sqrt{s} = 13$  TeV.

TABLE II: The yields  $10^{-6}$  of exotic states  $P_c^\pm(4312)$ ,  $P_c^\pm(4440)$  and  $P_c^\pm(4457)$  with three structures computed by PACIAE+DCPC model in  $pp$  collisions at  $\sqrt{s} = 7, 13$  TeV. Their parameter values  $\Delta m$  is taken as  $\Delta m = \Gamma/2 = 4.9$  MeV for  $P_c^\pm(4312)$ , as 10.3 MeV for  $P_c^\pm(4440)$ , and as 3.2 MeV for  $P_c^\pm(4457)$ . The value of decay width  $\Gamma$  is taken from LHCb experiment [9], respectively.

| $\sqrt{s}$ | bound state      | Particle      | Pentaquark ( $P_{cp}$ ) | Nucleus-like ( $P_{cn}$ ) | Molecular ( $P_{cm}$ ) | total            |
|------------|------------------|---------------|-------------------------|---------------------------|------------------------|------------------|
| 7TeV       | $J/\psi p$       | $P_c^+(4312)$ | $0.49 \pm 0.01$         | $1.79 \pm 0.04$           | $1.51 \pm 0.05$        | $3.79 \pm 0.10$  |
|            |                  | $P_c^+(4440)$ | $1.02 \pm 0.04$         | $3.71 \pm 0.10$           | $3.63 \pm 0.09$        | $8.34 \pm 0.17$  |
|            |                  | $P_c^+(4457)$ | $0.32 \pm 0.02$         | $1.12 \pm 0.04$           | $0.96 \pm 0.01$        | $2.39 \pm 0.05$  |
|            | $J/\psi \bar{p}$ | $P_c^-(4312)$ | $0.47 \pm 0.02$         | $1.75 \pm 0.04$           | $1.46 \pm 0.02$        | $3.68 \pm 0.08$  |
|            |                  | $P_c^-(4440)$ | $0.98 \pm 0.03$         | $3.63 \pm 0.09$           | $2.99 \pm 0.06$        | $7.60 \pm 0.19$  |
|            |                  | $P_c^-(4457)$ | $0.31 \pm 0.01$         | $1.11 \pm 0.02$           | $0.98 \pm 0.01$        | $2.39 \pm 0.03$  |
| 13TeV      | $J/\psi p$       | $P_c^+(4312)$ | $0.65 \pm 0.01$         | $2.29 \pm 0.03$           | $1.93 \pm 0.02$        | $4.87 \pm 0.04$  |
|            |                  | $P_c^+(4440)$ | $1.30 \pm 0.03$         | $4.80 \pm 0.06$           | $3.96 \pm 0.03$        | $10.05 \pm 0.07$ |
|            |                  | $P_c^+(4457)$ | $0.39 \pm 0.01$         | $1.48 \pm 0.01$           | $1.25 \pm 0.02$        | $3.11 \pm 0.01$  |
|            | $J/\psi \bar{p}$ | $P_c^-(4312)$ | $0.63 \pm 0.01$         | $2.30 \pm 0.03$           | $1.88 \pm 0.01$        | $4.82 \pm 0.05$  |
|            |                  | $P_c^-(4440)$ | $1.26 \pm 0.02$         | $4.73 \pm 0.05$           | $3.89 \pm 0.05$        | $9.88 \pm 0.03$  |
|            |                  | $P_c^-(4457)$ | $0.38 \pm 0.01$         | $1.46 \pm 0.03$           | $1.21 \pm 0.02$        | $3.06 \pm 0.03$  |

the molecular structure and pentaquark structure. Compared with  $J/\psi p$  cluster and  $J/\psi \bar{p}$  cluster, Fig.1 shows that  $J/\psi \bar{p}$  is slightly less than  $J/\psi p$ . We can conclude that in the PACIAE model, it is easier to generate  $P_c^+$  than antiparticle  $P_c^-$ . Furthermore, the yields of exotic states in  $\sqrt{s} = 13$  TeV is higher than those in  $\sqrt{s} = 7$  TeV,

showing there exists an evident energy dependence.

Note that, if the value of parameter  $\Delta m$  is determined, we can predict the yields of exotic states  $P_c$  from results in Fig.1. Here we take the parameter  $\Delta m$  as the half-decay width of the  $P_c \rightarrow J/\psi p$  mass spectrum, that is,  $\Delta m = \Gamma/2$ . The decay widths of the mass spectrum of

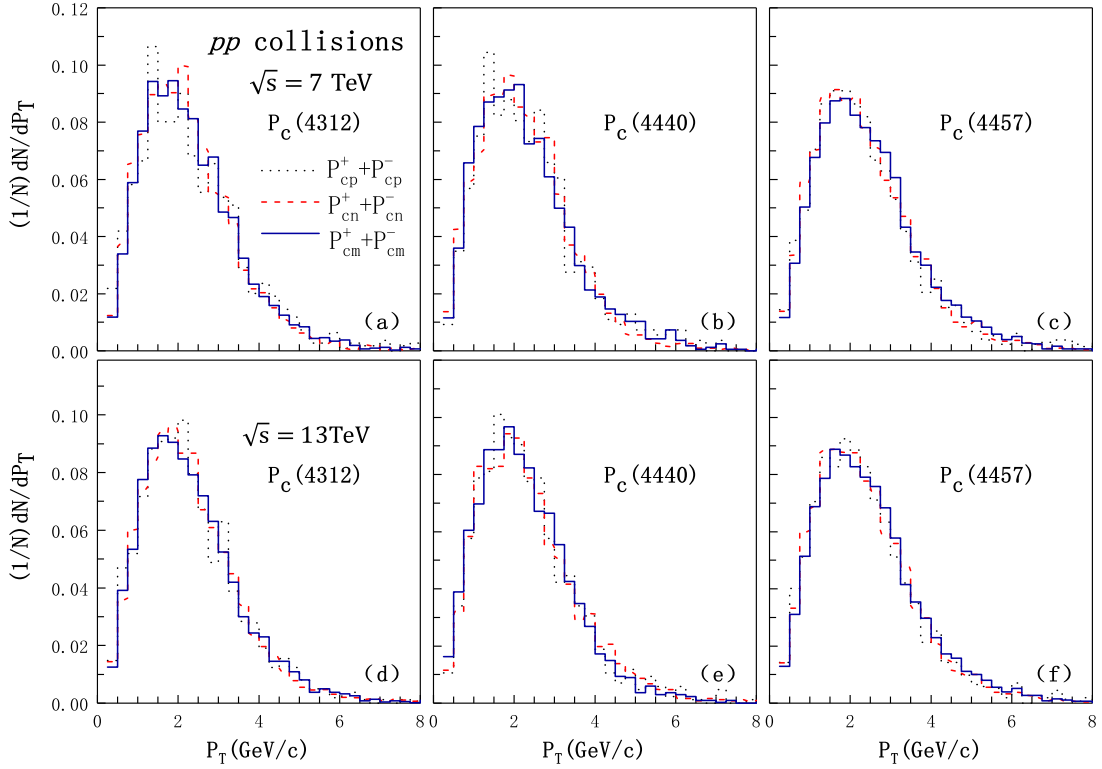


FIG. 2: The transverse momentum distribution of exotic states  $P_c^\pm(4312)$ ,  $P_c^\pm(4440)$  and  $P_c^\pm(4457)$  with three different structures ( $P_{cp}$ ,  $P_{cn}$ ,  $P_{cm}$ ) in  $pp$  collisions at  $\sqrt{s} = 7, 13$  TeV. The data are computed by using PACIAE+DCPC model. Three different structures exotic states of  $P_{cp}^\pm$ ,  $P_{cn}^\pm$ ,  $P_{cm}^\pm$  shown as black dotted, red dashed, and blue solid line, respectively. (a)  $P_c^\pm(4312)$  at  $\sqrt{s} = 7$  TeV, (b)  $P_c^\pm(4440)$  at  $\sqrt{s} = 7$  TeV, (c)  $P_c^\pm(4457)$  at  $\sqrt{s} = 7$  TeV, (d)  $P_c^\pm(4312)$  at  $\sqrt{s} = 13$  TeV, (e)  $P_c^\pm(4440)$  at  $\sqrt{s} = 13$  TeV, (f)  $P_c^\pm(4457)$  at  $\sqrt{s} = 13$  TeV.

$P_c^\pm(4312)$ ,  $P_c^\pm(4440)$ , and  $P_c^\pm(4457)$  from LHCb [9] are  $9.8 \pm 2.7^{+3.7}_{-4.5}$ ,  $20.6 \pm 4.9^{+8.7}_{-10.1}$  and  $6.4 \pm 2.0^{+5.7}_{-1.9}$  MeV, respectively. Then their parameter values  $\Delta m$  is taken as  $\Delta m = 4.9$  MeV for  $P_c^\pm(4312)$ , as 10.3 MeV for  $P_c^\pm(4440)$ , and as 3.2 MeV for  $P_c^\pm(4457)$ . Thus we can predict the yields of  $P_c^\pm(4312)$ ,  $P_c^\pm(4440)$  and  $P_c^\pm(4457)$  with three structures, as shown in Table 2. Overall, for the same exotic state  $P_c$ , the yield of molecular structure  $P_{cm}$  is slightly less than that of nucleus-like structure  $P_{cn}$ , is about three times as much as that of pentaquark structure  $P_{cp}$ . Obviously, the yields of positive ( $P_c^+$ ) and negative ( $P_c^-$ ) exotic particles are the same within the error. In the last column of Table 2, the total yields of the three different structure of  $P_c(4312)$ ,  $P_c(4440)$  and  $P_c(4457)$  particles produced in  $pp$  collisions at  $\sqrt{s} = 7, 13$  TeV are shown, we could predict the total yield is on the order of magnitude  $10^{-6}$ .

Fig.2 shows the transverse momentum distribution of three different mass exotic states of  $P_c^\pm(4312)$ ,  $P_c^\pm(4440)$  and  $P_c^\pm(4457)$  with three different structures ( $P_{cp}$ ,  $P_{cn}$ ,  $P_{cm}$ ) in  $pp$  collisions at  $\sqrt{s} = 7, 13$  TeV. The results are calculated by PACIAE+DCPC model. In each chart, the pentaquark structure, nucleus-like structure, and molecular structure are indicated by black dotted, red dashed, and blue solid line, respectively. From the

Fig 2, it can be seen that the transverse momentum distribution of the exotic states of  $P_c^\pm$  with three different mass of  $P_c^\pm(4312)$ ,  $P_c^\pm(4440)$ ,  $P_c^\pm(4457)$ , and three different structures of  $P_{cp}^\pm$ ,  $P_{cn}^\pm$ ,  $P_{cm}^\pm$  are all generally similar. When the collision energy increases from 7 to 13 TeV, the peak value of the traverse momentum of different exotic states  $P_c^\pm$  becomes slightly smaller, and the distribution becomes slightly wider.

The rapidity distributions of the exotic states  $P_c^\pm(4312)$ ,  $P_c^\pm(4440)$  and  $P_c^\pm(4457)$  with three different structures are computed by PACIAE+DCPC model in  $pp$  collisions at  $\sqrt{s} = 7, 13$  TeV, which are also presented in Fig.3. Obviously, one can see from Fig. 3 that there are symmetric distribution of rapidity distribution from -3 to 3. Here, rapidity distribution of the exotic states  $P_c^\pm$  with the different mass, structures, and collisions energy are all similar.

#### IV. CONCLUSIONS

In this paper, we use the PACIAE model to simulate the production of final state particles with the  $|y| < 3$ ,  $0 < p_T < 3$  GeV/c in  $pp$  collisions at  $\sqrt{s} = 7, 13$  TeV. Then by using DCPC model the exotic resonant state

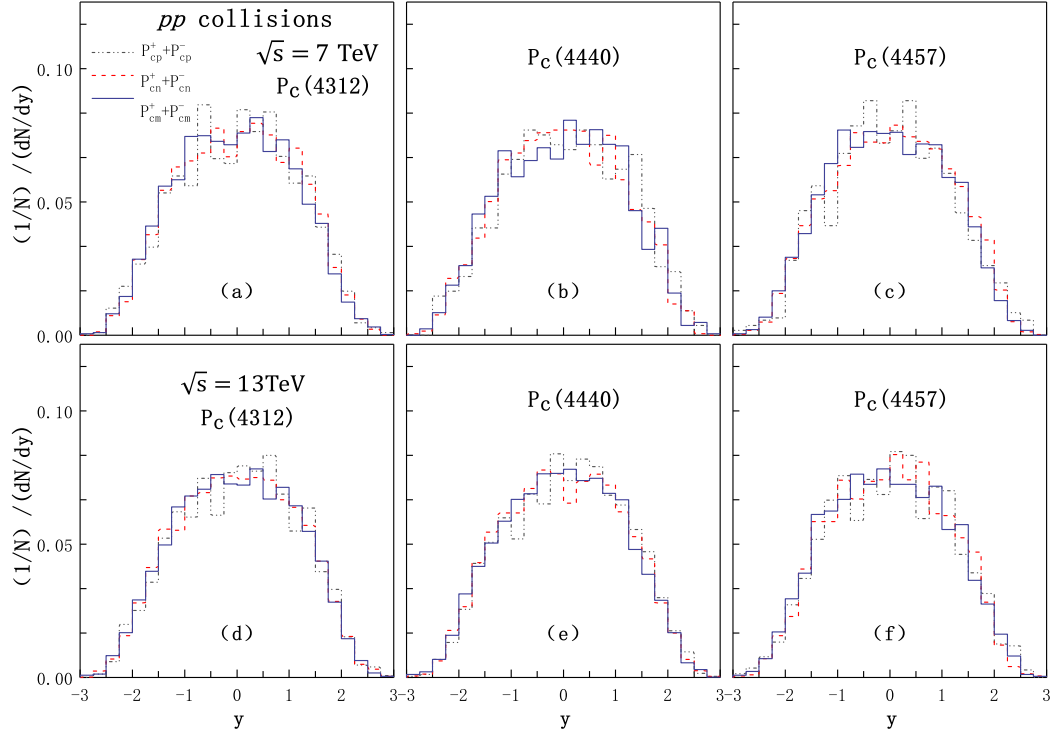


FIG. 3: The rapidity distributions of exotic states  $P_c^\pm(4312)$ ,  $P_c^\pm(4440)$  and  $P_c^\pm(4457)$  with three different structures ( $P_{cp}$ ,  $P_{cn}$ ,  $P_{cm}$ ) in  $pp$  collisions at  $\sqrt{s} = 7, 13$  TeV.

$P_c^\pm(4312)$ ,  $P_c^\pm(4440)$ , and  $P_c^\pm(4457)$  are investigated based on the decaying  $P_c^\pm \rightarrow J/\psi p(\bar{p})$ . We propose that the exotic state  $P_c^\pm(4312)$ ,  $P_c^\pm(4440)$  and  $P_c^\pm(4457)$  can be treated three possible structures of the pentaquark state ( $P_{cp}^\pm$ ), the nucleus-like state ( $P_{cn}^\pm$ ), and the molecular state ( $P_{cm}^\pm$ ). Taking the half-life of the mass spectrum as the mass uncertainty parameter,  $\Delta m = \Gamma/2$ , the yield of exotic states  $P_c^\pm(4312)$ ,  $P_c^\pm(4440)$ , and  $P_c^\pm(4457)$  with three kinds of structure are predicted in  $pp$  collisions at  $\sqrt{s} = 7, 13$  TeV, and the yield values are all on the order of  $10^{-6}$ . It is found that the yield of nucleus-like exotic states ( $P_{cn}^\pm$ ) are greater than that of molecular states ( $P_{cm}^\pm$ ), and the yield of molecular states ( $P_{cm}^\pm$ ) are greater than that of pentaquark ( $P_{cp}^\pm$ ). The yield of positive particles  $P_c^+$  is slightly larger than that of antiparticles  $P_c^-$ , but within the error range they are approximately equal. Their yield increases with the increase of collision energy, i.e., the yield of the exotic states  $P_c^\pm$  at  $\sqrt{s} = 7$  TeV is greater than that at  $\sqrt{s} = 13$  TeV. In addition, we study the transverse momentum distribution and the rapidity distributions of three exotic states  $P_c^\pm$  with different structures. It is found that the transverse momentum distribution and the rapidity distribu-

tions of the exotic state  $P_c^\pm$  with three different mass of  $P_c^\pm(4312)$ ,  $P_c^\pm(4440)$ ,  $P_c^\pm(4457)$ , three different structures of  $P_{cp}^\pm$ ,  $P_{cn}^\pm$ ,  $P_{cm}^\pm$ , and two different energies of 7, 13 TeV are all similar.

Finally, in order to find out further insight and understanding of the nature of the exotic resonant state  $P_c^\pm(4312)$ ,  $P_c^\pm(4440)$ , and  $P_c^\pm(4457)$ , we therefore suggest measurements of their production rates in  $pp$  and heavy-ion collisions by the ALICE and LHCb experiments.

#### Acknowledgments

The work of Y. L. Xie is supported by the National Natural Science Foundation of China (12005196) and the Fundamental Research Funds for the Central Universities (G1323519234), of D. M. Zhou is supported by the NSFC (11705167), and of G. Chen is supported by the National Natural Science Foundation of China (NSFC) (11475149).

**Data Availability Statement** This manuscript has no associated data or the data will not be deposited. [Authors' comment: The data used to support the findings of this study are available from the corresponding author upon request.]

- 
- [1] R. J. Jaffe, Phys. Rev. D **15**, 267 (1977); Phys. Rev. D **15**, 281 (1977); Phys. Rev. Lett. **38**, 195 (1977).  
 [2] D. Jido and T. Sekihara, Prog. Part. Nucl. Phys. **67**, 55

- (2012).  
 [3] J. Ho, D. Harnett and T.G. Steele, JHEP **1705**, 149 (2017).

- [4] M. Chanowitz and S. Sharpe, Nucl. Phys. B **222**, 211 (1983).
- [5] A. Pimikov, H.J. Lee and N. Kochelev et al., Phys. Rev. D **95**, 071501 (2017).
- [6] N. Brambilla, S. Eidelman and C. Hanhart et al., Phys. Rep. **873**, 1 (2020).
- [7] Y. -R. Liu, H. -X. Chen and W. Chen et al., Prog. Part. Nucl. Phys. **107**, 237 (2019).
- [8] R. Aaij et al. (LHCb Collaboration), Phys. Rev. Lett. **115**, 072001 (2015).
- [9] R. Aaij et al. (LHCb Collaboration), Phys. Rev. Lett. **122**, 222001 (2019).
- [10] M. -L. Du, V. Baru and F. -K. Guo et al., Phys. Rev. Lett. **124**, 072001 (2020).
- [11] F. -K. Guo, H. J. Jing and Ulf-G. Meißner et al., Phys. Rev. D **99**, 091501 (2019).
- [12] S. -Q. Kuang, L. -Y. Dai and X. -W. Kang et al., Eur. Phys. J. C **80**, 433 (2020).
- [13] A. Ali and A. Y. Parkhomenko, Phys. Lett. B **793**, 365 (2019).
- [14] M. I. Eides, V. Y. Petrov and M. V. Polyakov, Mod. Phys. Lett. A **35**, 2050151 (2020).
- [15] P. Zyla et al. (Particle Data Group), PTEP **2020**, 083C01 (2020).
- [16] H. -G. Xu, Z. -L. She and D. -M. Zhou et al., arXiv:2105.06261 (2021).
- [17] T. Sj östrand, S. Mrenna and P. Skands, JHEP **5**, 26 (2006).
- [18] B. -H. Sa, D. -M. Zhou and Y. -L. Yan et al., Comput. Phys. Commun. **183**, 333 (2012).
- [19] G. Chen, Y.-L. Yan and D. -S. Li et al., Phys. Rev. C **86**, 054910 (2012).
- [20] B. L. Combridge, J. Kripfganz and J. Ranft, Phys. Lett. B **70**, 234 (1977).
- [21] K. Stowe, An Introduction to Thermodynamics and Statistical Mechanics (Cambridge University Press, Cambridge, UK, 2007); R. Kubo, H. Ichimura, T. Usui, and N. Hashitsume, North-Holland, Amsterdam, 1965).
- [22] M. Wysocki, J. Phys. G: Nucl. Part. Phys. **31** S291 (2005).
- [23] R. Aaij et al. (LHCb Collaboration), Eur. Phys. J. C **71**, 1645 (2011).
- [24] J. Adam et al. (ALICE Collaboration), Eur. Phys. J. C **75**, 226 (2015).